Journal of Membrane Science 525 (2017) 359–367

Contents lists available at ScienceDirect

Journal of Membrane Science

journal homepage: www.elsevier.com/locate/memsci

Interpreting rejection in SRNF across grafted ceramic membranes through the Spiegler-Kedem model

Renaud B. Merlet[a], Cheryl R. Tanardi[a,b], Ivo F.J. Vankelecom[b], Arian Nijmeijer[a], Louis Winnubst[a,*,1]

[a] Inorganic Membranes, MESA+ Institute for Nanotechnology, University of Twente, P.O. Box 217, 7500 AE Enschede, The Netherland
[b] Centre for Surface Chemistry and Catalysis, Department of Molecular and Microbial Systems, KU Leuven, Kasteelpark Arenberg 23, P.O. Box 2461, 3001 Leuven, Belgium

ARTICLE INFO

Keywords:
Spiegler Kedem Katchalsky model
Organic solvent nanofiltration
PDMS
Grafting
Ceramic membranes, Gamma aluminum oxide

ABSTRACT

PDMS-grafted alumina membranes have already demonstrated high organic solvent permeabilities; described and modeled in this paper are their retention capabilities. In contrast to pure PDMS polymeric membranes, higher retentions were found in nonpolar solvents than in polar solvents. This is attributed to a solvent-induced pore-constriction behavior: confined swelling of PDMS, grafted into the membrane pores, was found to increase retention. To test this hypothesis, pore sizes were obtained by integrating the Ferry, Verniory and steric hindrance pore (SHP) equations into the Spiegler Kedem Katchalsky (SKK) model in order to predict the retention of dyes. Ultimately, a diffusion pore size was introduced into the SKK model to reflect the ability of the solute to diffuse through the swollen PDMS graft. A better understanding of the transport mechanisms that impact performance was achieved by incorporating the unique pore structure of these ceramic-based hybrid membranes into the SKK model.

1. Introduction

Solvent resistant nanofiltration (SRNF), also known as organic solvent nanofiltration (OSN), is a useful tool for separations in organic media, such as the removal of impurities from used solvents, recycling of solvents or the recovery of products from reaction mixtures in the chemical, petrochemical, and pharmaceutical industries [1,2]. For these kinds of applications, continuous exposure towards organic solvents is expected, which has generated a need for robust membranes. To meet this need, research has primarily focused on developing suitable polymeric membranes [3,4] rather than ceramic-based membranes. Polymeric membranes are more expensive but do not suffer from compaction effects or aging [5]. Consequently, the study of transport through SRNF membranes has also mainly dealt with polymeric membranes and the complex membrane-solvent-solute interactions that are unique to SRNF [6,7]. To enable process modelling and to facilitate the design of SRNF processes using ceramic-based membranes, the major parameters and transport mechanisms that influence the transport of solvents and solutes through the membrane must be quantified. This study investigates the retention behavior and transport mechanisms of a promising hybrid ceramic-based membrane in order to facilitate future applications of ceramic-based membranes for SRNF.

Membrane preparation by means of grafting polymer chains into the pores of a rigid ceramic membrane offers the opportunity to integrate pore size tuning and surface wettability/functionality into a single modification step, while avoiding the effects of swelling and aging typically experienced by purely polymeric membranes. Several instances of porous inorganic membranes modified by grafting have been employed in various applications [8–13] demonstrating the potential for grafting as a method to prepare selective and chemically stable membranes.

However, to date only a few studies have attempted to elucidate the rejection behavior of ceramic membranes for OSN. One such study dealt with a purely ceramic membrane, a ZrO_2/TiO_2 hydrophobic membrane produced by a modified sol-gel technique and pyrolysis in an inert atmosphere [14]. A modified pore-flow model, based on the work of Bowen and Welfoot [15], was used to describe the transport through these membranes [16], though the model was found to be valid for only one solvent, THF. Another type of ceramic membrane, produced by Hosseinabadi et. al. [17], consists of short alkyl and phenyl oligomers which were Grignard-grafted into the pores of 1 nm

* Corresponding author.
E-mail address: a.j.a.winnubst@utwente.nl (L. Winnubst).
[1] www.utwente/tnw/im

http://dx.doi.org/10.1016/j.memsci.2016.12.013
Received 24 July 2016; Received in revised form 8 December 2016; Accepted 10 December 2016
Available online 12 December 2016
0376-7388/

TiO_2 and 3 nm ZrO_2 membranes. This reaction yielded a partial surface coverage, giving the membranes an amphiphilic character and high selectivity in various organic solvents. The transport of polyethylene glycol (PEG) and polystyrene (PS) oligomers in a variety of solvents was explained by fitting the Spiegler Kedem model to the retention data [18]. Those solvents were divided into two classes: (1) those with low polarity, experiencing low retentions varying with pressure; and (2) those with high polarity, experiencing high retentions independent of pressure. It was concluded that solutes in high polarity solvents are transported mainly by convection, implying a size-rejection mechanism. Solute transport in low polarity solvents was concluded to be significantly impacted by diffusion, meaning the applied pressure and polarity of solutes played a role in rejection.

Unlike the ceramic membranes used by Blumenschein et al. or Hosseinabadi et al., the membranes investigated here have been modified by the immobilization of short PDMS chains into the 5 nm pores of γ-Al_2O_3 membranes. Modified in this way, the alumina membrane retains its porous character; its pores are shrunken and now suited to SRNF due to their newfound hydrophobicity. When in contact with a solvent, the PDMS can only swell away from the pore wall, towards the center of the pore, effectively shrinking the pore. The benefit of confining PDMS is apparent when compared against a "free" PDMS polymeric membrane. When in contact with a highly-swelling solvent, free PDMS membranes showed reduced retention and increased permeability [19], while PDMS-grafted alumina membranes showed decreased permeability [20].

Tanardi et. al. [20] identified solvent viscosity and the effect of solvent sorption as the major parameters influencing the transport of pure solvents through PDMS-grafted 5 nm γ-Al_2O_3 membranes. Specifically, solvent permeation through these membranes was described as following a pore flow behavior, and a linear relationship between graft sorption and viscosity-corrected membrane permeability was established. This relationship between swelling and permeability is illustrated in Fig. 1. Unlike pure ceramic or Grignard-functionalized membranes, PDMS-grafted alumina membranes have demonstrated a distinct, quantifiable response to solvent-induced pore swelling. This fundamental difference merits a separate investigation and analysis into the retention behavior of PDMS-grafted 5 nm γ-Al_2O_3 membranes, which is precisely the aim of this work.

Gamma-alumina with a native pore size of 5 nm was grafted with two PDMS graft sizes, whose lengths are defined by their number-average of repeating monomer units, n=10 or n=39. First, Sudan Black B was chosen as a probe solute, and its retention in seven different organic solvents as a function of pressure was collected and analyzed. The impact of feed pressure on dye rejection is discussed, followed by an estimation of the pore size for each membrane. It should be emphasized that the term "pore size" refers here to the openings created by the rapidly moving grafted polymer chains, which can be physically interpreted as the average diameter of the free volume elements represented as a cylinder. Subsequently, dyes varying in molecular weight were tested in a hydrophilic (isopropanol) and a hydrophobic (toluene) solvent to investigate the effect of solvent-membrane affinity on the observed membrane rejection. Throughout, the applicability of the Spiegler-Kedem-Katchalsky (SKK) model as a solute rejection model to accurately describe the rejection behavior of the PDMS-grafted ceramic membranes is considered. A modification to the SKK model is made to accommodate the unique characteristics of these membranes. The resulting model agrees well with the experimental data.

2. The Spiegler-Kedem-Katchalsky solute transport model

A general model to describe solute transport for both porous and nonporous membranes is given by Kedem and Katchalsky [21], in which the membrane is considered a black box, comprising a feed and a permeate as the input and output, respectively. The flux of the solute through the membrane is described as:

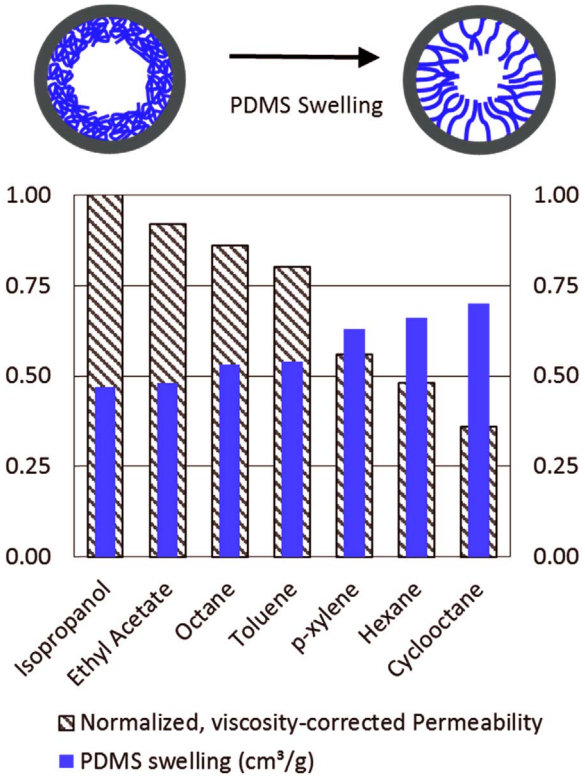

Fig. 1. Normalized, viscosity-corrected permeabilities of the M2 membranes and PDMS sorption data for different solvents [20]. Specific values can be found in Table 1. Accompanying the graph is a conceptual diagram of a PDMS-grafted pore (top-down view) in contact with a weakly-swelling solvent (left) and a strongly-swelling solvent (right). cm^3/g.

$$J_c = P_c \Delta x \frac{dc}{dx} + (1 - \sigma) J_v \bar{c} \quad (1)$$

where J_c is the solute flux, P_c the solute permeability, Δx the membrane thickness, $\frac{dc}{dx}$ the concentration gradient over the membrane, σ the reflection coefficient, which is a measure of the selectivity of the membrane towards a specific solute, $\bar{c}$ the logarithmic average of the solute concentration over the membrane and $J_v$the solvent flux. The solvent flux is defined as:

$$J_v = \Delta P^* k_v \quad (2)$$

where k_v is the membrane permeability, specific to a solvent, and ΔP the difference between the feed and permeate pressure, also termed the trans-membrane pressure (TMP). In Eq. (1), the first term describes the transport of solutes by a diffusion mechanism, while the second term describes the transport of solutes by a convection mechanism.

The rejection, R, of a solute is obtained experimentally by the following classic equation:

$$R = 1 - \frac{c_p}{c_f} \quad (3)$$

where c_p and c_f are the solute concentrations in permeate and feed solution, respectively.

From Eqs. (1)–(3), Spiegler and Kedem derived the following two equations to predict rejection [22,23]:

$$R = \frac{\sigma(1 - F)}{1 - \sigma F} \quad (4)$$

where F (the flow parameter) is:

$$F = \exp\left(\frac{\sigma - 1}{P_c} J_v\right) \quad (5)$$

These equations are a function of the solvent flux, the reflection coefficient, and the solute permeability. Hereafter, Eqs. (1), (4) and (5) will be referred to collectively as the SKK (Spiegler-Kedem-Katchalsky) model.

Originally termed a flow parameter, F indicates which solute transport mechanism, convection or diffusion, is dominant, if any. Since J_v scales with feed pressure but P_c does not, the applied pressure across the membrane will affect the solute rejection. As the pressure increases, F tends towards zero, and solutes are transported by convective flow rather than by diffusion, so:

$$\frac{J_v}{P_c} \to \infty;\ F \to 0;\ \sigma \to R \tag{6}$$

While operating in the convective regime, as defined in Eq. (6), the rejection is solely dependent on the reflection coefficient, and is constant for a membrane-solvent pair. However, when F is not near to zero, both the effects of diffusive and convective transport must be taken into account, and rejection remains a function of several parameters as shown in Eq. (7).

$$R = F(Jv, Pc, \sigma) = F(\Delta P, k_v, P_c, \sigma) \tag{7}$$

Hence, whether or not experimental rejection values vary with applied pressure will indicate whether the diffusion of solutes across the membrane is influencing membrane performance.

2.1. The convection term

As ΔP increases, the solvent flux increases, and F tends to 0. As described above, the reflection coefficient will then equal rejection (Eq. (6)), i.e. the convection mechanism becomes dominant and diffusion can be neglected at sufficiently high pressures. The reflection coefficient can then be determined from a simple rejection experiment. This coefficient is related to the ratio of the solute diameter to the pore diameter through the three established models described below.

First, Ferry [24] proposed a solute transport model, which relates the reflection coefficient to the ratio of solute diameter to pore diameter. This model shows increasing rejection as the solute size nears the pore size, and solutes of a larger diameter than the membrane pore diameter are completely rejected. The membrane is assumed to be isoporous, and no interactions between the membrane, solvent and solute are taken into account. Therefore, the pore size obtained in this way is hence no more than the effective radius of an ideal filtration. The reflection coefficient develops from 0 to 1 as the ratio of d_c/d_p increases from 0 to 1, where d_c is the average solute diameter and d_p the mean pore diameter. This means $\sigma=1$ when $d_c/d_p \geq 1$ and $\sigma=0$ when $d_c/d_p = 0$. Ferry's model can be expressed in the following way:

$$\sigma = \left(\frac{d_c}{d_p}\left(\frac{d_c}{d_p} - 2\right)\right)^2, \quad \left\{\frac{d_c}{d_p} \in \quad 0 \leq \quad \frac{d_c}{d_p} \leq 1\right\} \tag{8}$$

Second, the Verniory model [25] incorporates wall friction forces occurring between the solute and membrane pore surface, meaning that a given solute particle size is predicted to experience a higher rejection than the Ferry model. The Verniory model can be written as:

$$\sigma = 1 - \left(\frac{1 - \frac{2}{3}\frac{d_c}{d_p}^2 - \ 0.2\frac{d_c^5}{d_p^5}}{1 - \ 0.76\frac{d_c^5}{d_p^5}}\right)\left(1 - \frac{d_c}{d_p}\right)^2\left(2 - (1-\frac{d_c}{d_p}\right)^2,$$

$$\left\{\frac{d_c}{d_p} \in \quad 0 \leq \quad \frac{d_c}{d_p} \leq 1\right\} \tag{9}$$

Third, the steric hindrance pore (SHP) model [26] accounts for a rejection case in which attractive forces between membrane and solute are assumed. Consequently, lower rejections would be calculated for a given solute size than the Ferry size-exclusion model. The SHP model is expressed as:

$$\sigma = 1 - \left(1 + \frac{16}{9}\frac{d_c}{d_p}^2\right)\left(1 - \frac{d_c}{d_p}\right)^2\left(2 - (1-\frac{d_c}{d_p}\right)^2,$$

$$\left\{\frac{d_c}{d_p} \in \quad 0 \leq \quad \frac{d_c}{d_p} \leq 1\right\} \tag{10}$$

The three reflection coefficient models described above assume three different solute-membrane interactions. These models were chosen to screen for significant interactions, other than size-exclusion, that influence the reflection coefficient. Though coupling the reflection coefficient to the ratio of solute diameter to pore diameter prevents the prediction of negative rejections, we expected no negative rejections given the relatively inert nature of the pore surface (PDMS) and solutes (neutral dyes). Using these three models, three similar pore sizes were obtained from each of the rejection data of various solute-solvent pairs, as presented in Section 4.

2.2. The diffusion term

Here, the solute permeability can be taken as being equal to the diffusivity of the solute through the membrane pore over the thickness of the separation layer [27]:

$$P_c = \frac{D_c}{\Delta x} \tag{11}$$

where Δx is the thickness of the separation layer and D_c the diffusion coefficient of the solute through the pore. The Stokes-Einstein relation predicts an inverse relationship between the solute diameter and its diffusion coefficient as shown in Eq. (12).

$$D_c = \frac{kT}{3\pi\mu d_c} \tag{12}$$

where μ is the viscosity, and T the temperature. Van der Bruggen et al. [28] developed a simplification of Eqs. (11) and (12) by extracting the solute diameter, d_c, from Eq. (12) and combining the remainder of the diffusivity term and separation layer thickness into one diffusion parameter, ω. This parameter was then applied to the SKK model in order to describe the retention of uncharged solutes in aqueous media as a function of solute size, as shown in Eq. (13).

$$P_c = \frac{\omega}{d_c} \tag{13}$$

where ω is empirically determined, specific to a solvent-membrane pair at a constant temperature, and is readily obtainable once the reflection coefficient is known.

Once the reflection coefficient (σ) is obtained, two pieces of information are then available: a pore size from either the Ferry, Verniory or SHP models and the solute permeability parameter, ω. This parameter (ω) allows for a prediction of rejection of other solute diameters through the same solvent-membrane combination by changing the solute diameter, d_c, in Eq. (13). However, the filtration experiment may not be operating in the convection-only regime. In that case, it is possible to determine σ by extrapolating the rejection versus pressure curve to an area of higher applied pressure, in which the rejection becomes constant as the solvent flux increases relative to the pressure-independent solute permeability.

The discussion of this work describes the applicability of the SKK model to describe the solute rejection behavior of two types of γ-alumina membranes grafted with either a short or long PDMS chain (n=10 or n=39). Reflection coefficients are either obtained directly from rejection vs pressure experiments, or the data are extrapolated to a region of steady rejection. From these reflection coefficients, pore sizes are calculated using the Ferry, SHP and Verniory model. Once the reflection coefficient is known, ω is calculated, and rejection predictions are then made for various sized solutes in both toluene and isopropanol.

3. Materials and methods

Two types of polydimethylsiloxane (PDMS)-grafted ceramic membranes were studied. The first series of membranes (M1) consisted of macroporous α-Al_2O_3 supports, topped with a 0.3 μm thick mesoporous (pore size 5 nm) γ-Al_2O_3 layer which was modified with 3-aminopropyltriethoxysilane (APTES) followed by mono(2,3-epoxy) polyetherterminated polydimethylsiloxane (n=10). Details of the membrane modification procedure are described elsewhere [29]. The second series of membranes (M2) consisted of macroporous α-Al_2O_3 supports, topped with an identical 0.3 μm thick mesoporous (pore size 5 nm) γ-Al_2O_3 layer which was modified by using mercaptopropyl triethoxysilane (MPTES) followed by monovinyl terminated polydimethylsiloxane (n=39). Details of this membrane modification procedure can be found in [27]. All membranes were flat discs with a diameter of 20 mm and a thickness of 2.5 mm. The mean pore diameters of the unmodified, APTES-grafted, and MPTES-grafted γ-Al_2O_3 were obtained by permporometry using cyclohexane as condensable gas [8].

The solvents, namely octane (98% purity), cyclooctane (> 99%), p-xylene (> 99%), and n-hexane (> 99%) were purchased from Sigma-Aldrich. Toluene (100%), ethloyl acetate (99.9%), and isopropanol (100%) were purchased from VWR. All solvents were dried using zeolite A (molecular mesh 4–8 nm) purchased from Sigma-Aldrich and pretreated for 1 h at 200 °C. Dyes were purchased from Sigma-Aldrich, and their chemical structures are shown in Fig. 2.

Filtration experiments were performed using a stainless steel dead-end pressure cell. This cell was filled with feed solution and nitrogen was used to pressurize the cell. The feed solution was continuously stirred at a speed of 500 rpm. Filtration experiments were performed at each TMP at 50% recovery. Before each test, the membranes were soaked for 24 h in the solvent to be tested. Between each rejection test, the setup was thoroughly cleaned and the membranes were rinsed with the previous solvent and then cleaned in an ultrasonic bath of fresh ethanol for 10 min. After this cleaning treatment, the membranes were dried in a vacuum oven at 80 °C for 24 h before the next test.

The nanofiltration behavior of Sudan Black B was investigated for all solvents. All other dyes (except Rose Bengal) were studied in both toluene and isopropanol. However, Rose Bengal was only studied in isopropanol, due to its insolubility in toluene. The feed solutions consisted of 8000 ppm of dye. All measurements were performed on three different samples for each type of membrane with three measurements per sample.

Dye solute concentrations in the feed and permeate solution were analyzed using a Perkin-Elmer ʎ12 UV–vis Spectrophotometer. The rejection (R) was calculated by the following equation: $R=(1-C_p/C_f)$ x100%, where C_p and C_f are the solute concentrations in permeate and feed solution, respectively. C_f and C_p were determined as a function of total area from a plot of electric potential versus time. To check whether any concentration polarization occurs, the solvent permeation of blank feeds (pure solvents without solutes) and those with solutes were compared using a similar set-up. Permeate fluxes were obtained by measuring the weight of the collected permeate as a function of time. It should be noted that no significant differences were observed between the permeation of blank feeds [20] and those with solutes, suggesting that no concentration polarization of solutes occurred during the measurements.

The average molecular diameter of the dye solutes (d_c) were calculated by using the *CS 3D Model* software by taking into account the bond length, the corresponding Van der Waals radius, and the bond angle as given in [30,31]. Since the dye solute can be positioned in various conformations when approaching the membrane pores and assuming that the different conformations may have a similar probability of occurring [32], an average value for each type of dye is used, representing the average size of the solute molecular diameter in the axial, horizontal and lateral direction. These values are given in Fig. 2.

4. Results and discussion

4.1. The impact of pressure & graft swelling on rejection

Fig. 3 shows rejection data of Sudan Black B in various solvents as a function of trans-membrane pressure. Please note that plotting rejection against applied pressure and not solvent flux is in order to be able to compare the seven solvents in one figure. It can be seen that, for most cases, dye rejection increased with applied pressure regardless of the type of solvent used. The possibility of deformation (e.g. shear-induced compaction) of the graft under the pressures tested has been discarded, as this would result in a larger membrane pore diameter at higher applied pressures, consequently decreasing rejection and increasing solvent permeability. This is in agreement with the previous observation on the same type of membranes: an absence of shear rate flow induced behavior is attributed to the unyielding nanostructure of

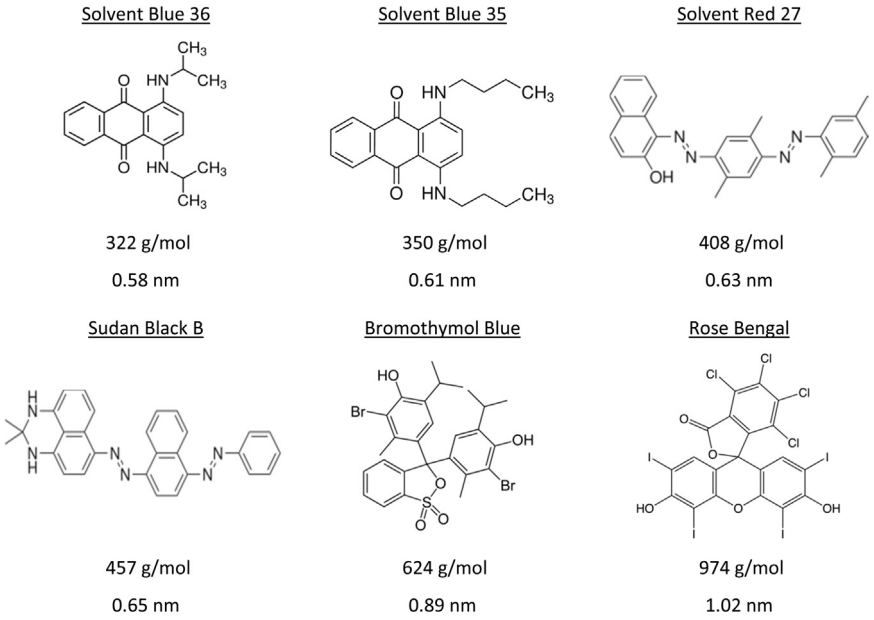

Fig. 2. The chemical structures, molar masses and diameters of the dyes used.

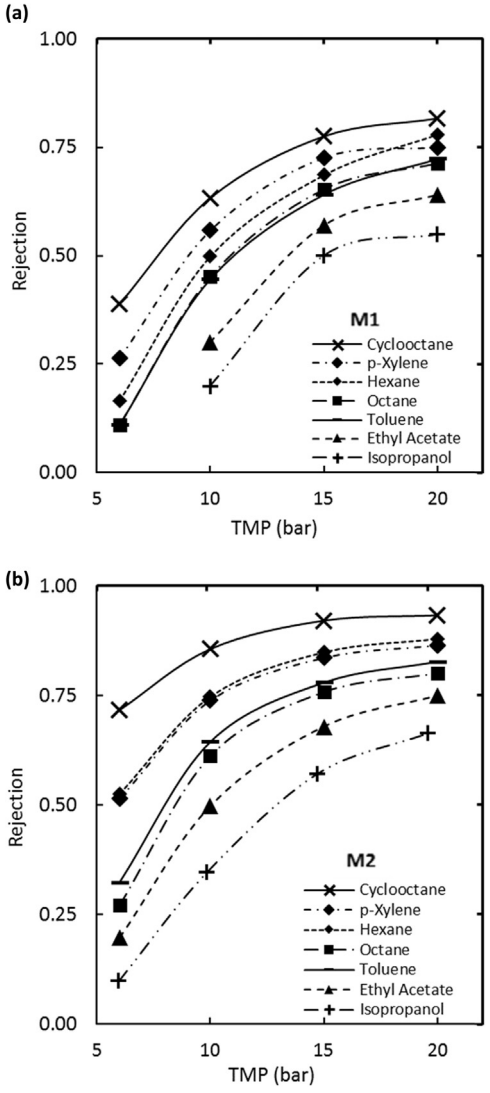

Fig. 3. Rejection of Sudan Black B in different solvents versus TMP at room temperature for (a) M1 and (b) M2 membranes.

the rigid ceramic substrate over the pressure range studied [20].

It can be observed in Fig. 3 that rejections of Sudan Black B varied according to the solvent used. The highest rejection of Sudan Black B was found in cyclooctane, while the lowest rejection was found in isopropanol. In Table 1, the specific rejection values (R) of Sudan Black B at a TMP of 20 bars for M1 and M2 membranes are given. To gauge whether there is a relation between rejection and solvent viscosity, viscosity values are also given in Table 1. Another factor which can influence the rejection is the degree of graft swelling, which is a function of the permeating solvent. A measure of polymer swelling is the solvent sorption (S) by the polymer (PDMS) as defined in [20] and therefore, corresponding solvent sorption values are given in Table 1.

In a previous study, pure solvent permeation was studied on these same membranes [20]; the permeability data are provided in Table 1. In that study, it was shown that both solvent viscosity and sorption of solvent into the grafted moiety determine solvent transport through the membrane. It is logical that the swollen graft does not only influence the solvent transport, but also the solute rejection of the membrane. In this case, the relatively stronger sorption of cyclooctane in the grafted moiety compared to that of isopropanol would be expected to result in a smaller pore size in the presence of cyclooctane, thus yielding a higher solute rejection in cyclooctane than in isopropanol.

For free (or unconfined) PDMS polymeric membranes, lower rejections are observed in the presence of toluene whereas higher rejections are observed in the presence of isopropanol [33–35]. However. the results of this work, as partially summarized in Table 1, show the opposite behavior, meaning a higher solute rejection in toluene than in isopropanol for both types of PDMS grafted ceramic membranes (M1 and M2). This again emphasizes the different behaviors of a “free” PDMS membrane compared to that of membranes in which PDMS is confined to a ceramic matrix. For an unconfined PDMS membrane, the sorption of solvent leads to free swelling, thus a more open membrane structure, while for grafted ceramic membranes, it is suggested that a strongly sorbed solvent leads to a more closed structure of the grafted membranes [20]. This explains the higher solute rejection in the presence of toluene than in the presence of isopropanol.

It can be further observed from Fig. 3 that rejection increases nonlinearly with TMP regardless of the type of solvent used. From Fig. 3b, it can be seen that the strongly swelling solvents reach a region of constant rejection; for instance, the change in rejection of Sudan Black B in cyclooctane and p-xylene, by increasing TMP from 15 to 20 bar, is less than the experimental error (± 1). The other solvent-membrane pairs given in Fig. 3 do not reach this rejection plateau, but do however seem to trend towards a constant rejection value at TMP > 20 bar.

These observations are in agreement with the traditional SKK model: if the diffusion of solutes is independent of pressure, and thus becoming negligible at higher solvent flux, then according to the SKK model the effect of convection becomes dominant. At these feed pressures, the relationship between solute flux and solvent flux becomes constant and thus rejection trends towards a constant value equal to the reflection coefficient, as given in Eqs. (4) and (5). As previously mentioned, some solvent-membrane combinations reached this constant rejection value; for example, Sudan Black B rejection reached a limiting value of 92% for cyclooctane in M2 (Fig. 3b). It can therefore be assumed that this value is equal to the reflection coefficient of Sudan Black B in cyclooctane for membrane M2.

For those solvent-membrane pairs that did not reach a constant rejection value, the existing data points of Fig. 3 are an input into Eqs. (4) and (5), and by least-squares fitting (here done using Matlab R2014b) reflection coefficients (σ) are obtained. These σ values, listed

Table 1
The rejection (R) of Sudan Black B in different solvents for M1 and M2 membranes at TMP of 20 bar at 50% recovery along with solvent properties and permeabilities from [20].

Solvent Types	μ[a] (mPa s)	S[b] V_s (cm^3/g)	J_{M1}[b] ($Lm^{-2} h^{-1}$ bar^{-1})	J_{M2}[b] ($Lm^{-2} h^{-1}$ bar^{-1})	R_{M1} (%)	R_{M2} (%)
Isopropanol	2.39	0.47	0.9 ± 0.1	0.8 ± 0.1	55 ± 1	66 ± 1
Ethyl acetate	0.45	0.48	4.6 ± 0.1	3.7 ± 0.1	64 ± 1	75 ± 1
Octane	0.54	0.54	3.4 ± 0.1	2.9 ± 0.1	71 ± 1	80 ± 1
Toluene	0.59	0.53	3.1 ± 0.1	2.5 ± 0.1	72 ± 1	83 ± 1
p-xylene	0.64	0.63	2.7 ± 0.1	1.6 ± 0.1	75 ± 1	87 ± 1
Hexane	0.31	0.66	4.8 ± 0.1	2.8 ± 0.1	78 ± 1	88 ± 1
Cyclooctane	2.13	0.70	0.6 ± 0.1	0.3 ± 0.1	82 ± 1	93 ± 1

[a] Solvent viscosity (at 20 °C).
[b] Sorption and permeability values from [20].

Table 2
Membrane pore diameters (d_p , in nm) for membrane M1 and M2, calculated from the Ferry, SHP and Verniory models. The reflection coefficients (σ) for membrane-solvent pairs, used for these calculations, are also shown.

Solvent	M1				M2			
	σ	d_p (nm)			σ	d_p (nm)		
		SHP	Ferry	Verniory		SHP	Ferry	Verniory
Isopropanol	0.54	0.96	1.31	1.43	0.82	0.75	0.82	0.87
Ethyl acetate	0.65	0.90	1.14	1.24	0.85	0.73	0.80	0.84
Toluene	0.79	0.79	0.91	0.97	0.88	0.73	0.79	0.83
Octane	0.77	0.81	0.95	1.02	0.85	0.75	0.83	0.88
p-Xylene	0.78	0.80	0.93	0.99	0.88	0.75	0.82	0.87
n-Hexane	0.81	0.78	0.89	0.95	0.90	0.72	0.78	0.81
Cyclooctane	0.83	0.77	0.87	0.93	0.92	0.71	0.76	0.79

in Table 2, were then used to calculate the membrane pore size characteristic of each solvent using the SHP, Ferry and Verniory models. Each solvent-membrane pair therefore yields three pore sizes for each membrane, as shown in Table 2. The most precise approximations of σ are obtained for those solvent-membrane pairs whose rejection data are at their high-pressure plateau. As expected from the permeability and swelling data, given in Table 1, the pore sizes are inversely proportional to the degree of graft swelling.

The pore diameters listed in Table 2 were compared to pore sizes obtained through other characterization methods. The mean pore diameter of the native (non-grafted) γ-Al_2O_3 was confirmed to be 5.0 ± 0.1 nm as measured by permporometry. The pore diameter was found to be shrinking to 3.0 ± 0.1 nm post-linker grafting for both M1 (APTES linker) and M2 (MPTES linker). Previous analysis [36,37] of nitrogen adsorption/desorption isotherms on the native, linker-grafted and PDMS-grafted γ-alumina flakes gave the pore diameters in dry (solvent-free) conditions. Uniform pores were observed that had estimated pore diameters of 4.8 nm for native γ-alumina, 4.2 nm post-APTES grafting, 2.2 nm for the grafted M1 γ-alumina flakes and 1.8 nm for the grafted M2 γ-alumina flakes. As expected, the wet pore sizes given in Table 2 are markedly smaller than the native γ-Al_2O_3 pore sizes, also smaller than the linker-grafted pore size, and smaller than the dry-PDMS pore sizes.

4.2. Rejection vs. solute diameter: dyes

The rejection of several dyes was studied in toluene and isopropanol for both membranes (M1 and M2), and a summary of the results can be found in Table 3. In the previous section, the rejection of Sudan Black B in both toluene and isopropanol at a TMP of 10 bar was found to be in the mixed diffusion-convection regime. Therefore, it was expected that the rejection predictions and rejection data treated in this section would also be in the mixed diffusion-convection regime. To calculate the expected rejection, both the reflection coefficient (σ) and solute permeability (P_c) were calculated as a function of solute size for each membrane-solvent pair tested.

Table 3
Hydrodynamic diameters (d_c) of various dye solutes and the experimental rejection values at TMP =10 bars in toluene or isopropanol for membranes M1 (= R_{M1}) and M2 (=R_{M2}).

Solutes	d_c (nm)	Toluene		Isopropanol	
		R_{M1} (%)	R_{M2} (%)	R_{M1} (%)	R_{M2} (%)
Solvent blue 35	0.58	40 ± 1	55 ± 1	16 ± 1	28 ± 1
Solvent blue 36	0.61	44 ± 1	60 ± 1	18 ± 1	31 ± 1
Solvent red 27	0.63	46 ± 1	62 ± 1	19 ± 1	33 ± 1
Sudan black B	0.65	45 ± 1	64 ± 1	20 ± 1	35 ± 1
Bromothymol blue	0.89	65 ± 1	81 ± 1	31 ± 1	53 ± 1
Rose bengal	1.02	–	–	40 ± 1	65 ± 1

The values of σ and P_c were related to values of d_p and ω, respectively, as a function of solute and pore diameter using the Ferry, SHP and Verniory models (Eqs. (8)–(10)) and the diffusion permeability (Eq. (13)). The pore size and diffusion parameter were obtained from the Sudan Black B rejection versus pressure data presented in the previous section. Since three pore sizes were obtained (Table 2), three sets of rejection values were predicted, from d_c/d_p =0 up to d_c/d_p =1. The solvent permeabilities of membranes M1 and M2 are already known [20] for each solvent-membrane pair. Applying these data, comparisons between experimental and predicted rejection values were made, as shown in Fig. 4, a to d.

The results shown in Fig. 4 show that rejection is generally higher in toluene than in isopropanol, which is to be expected from the impact of swelling as previously discussed. Also expected were the higher rejections caused by M2 than M1 in the same solvent, because the pores of M2 are smaller because of the larger PDMS monomer used (n=39 versus n=10 for M1). Finally, and in accordance with the general behavior of porous membranes, the rejection of dyes is largely a function of their molecular size, and hence of their molecular weight. However, the SKK model predictions are not in accordance with the experimentally observed results on two points specifically: solutes bigger than the calculated pore size are able to permeate through the membrane, and 100% rejection is not reached at the proposed pore size. For example, the SHP pore diameters of M1 and M2 in isopropanol were calculated to be 0.96 nm and 0.75 nm, respectively, and the diameter of Rose Bengal is 1.02 nm and yet its rejections are below 70% for both M1 and M2. To address these issues, we further discuss the unique pore structure of these grafted ceramic membranes. Membranes M1 and M2 benefit from a rigid ceramic architecture, constraining the swelling of the grafted PDMS chains. However, PDMS, especially when swollen, is not a dense material, nor is the interface between the solvent grafted chains especially hard or well-defined [38]. Diffusion of solutes through the membrane has until now been assumed to be subject to the same reduced pore size as the convection of solutes and solvents, but now it can reasonably be assumed the solute can permeate through the free space between the grafted PDMS chains. The remainder of this section describes the integration of a pore size for diffusion (d_d) into the SKK model.

The diffusion pore size (d_d) is larger than the convection pore size (d_p) for these ceramic-based hybrid membranes. Since a portion of the solute is able to diffuse through the swollen graft, effectively increasing the apparent pore size for the diffusion mechanism, solutes larger than the convection pore diameter are allowed to permeate through the membrane. The diffusion pore size is taken to be equal to the pore diameter before the grafting of PDMS, measured by permporometry as 3.0 nm ± 0.1 for both M1 (APTES linker) and M2 (MPTES linker), as shown in Table 4.

The fact that the modeled retentions, as given in Fig. 4, do not reach unity when the pore size equals the solute size is due to the incorporation of the Stokes-Einstein equation to calculate P_s as a function of pore size (Eqs. (11)–(13)). In this case free diffusion is assumed, i.e. diffusion of solutes is unhindered by the pore walls. To account for the hindrance caused by the pore wall, the Renkin equation is used. This expresses the ratio of hindered diffusion, D_c^*, to free diffusion (D_c, Eq. (12)) of a spherical particle inside a cylinder of known diameter as a function of the ratio of solute to cylinder diameter. Since its introduction in 1954 [39], agreement with experimental data has been observed for both biological and non-biological membranes [40–42]. The Renkin equation is below:

$$\frac{D_c^*}{D_c} = f\left(\frac{d_c}{d_d}\right) = \left(1 - \frac{d_c}{d_d}\right)^2 \left(1 - 2.104\left(\frac{d_c}{d_d}\right) + 2.09\left(\frac{d_c}{d_d}\right)^3 - 0.95\left(\frac{d_c}{d_d}\right)^5\right) \quad (14)$$

Now a new permeability (P_c^*) incorporates d_d through the Renkin equation as shown in Eq. (15).

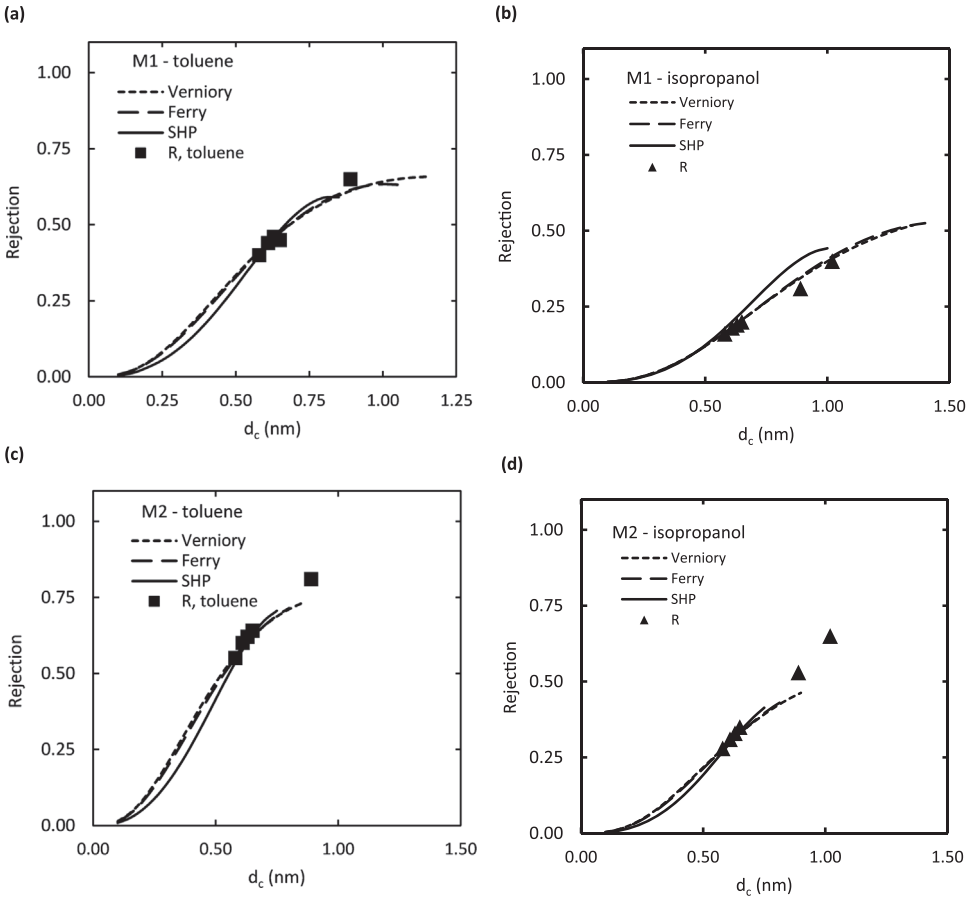

Fig. 4. Comparison of experimental dye rejection as function of d_c for M1 in (a) toluene and in (b) isopropanol and for M2 in (c) toluene and (d) isopropanol with the predicted SKK rejection values from the Verniory, Ferry and SHP pore sizes. Points represent experimental data; lines the SKK model.

Table 4
The ω and d_d values of M1 and M2 used in rejection predictions. The ω value is the diffusion parameter, and the diffusion pore diameter (d_d) is the diameter of the pore after organosilane (linker) attachment, as determined by permporometry. This value does not vary significantly from M1 to M2.

Solvent	ω (L m^{-1} h^{-1})		d_d (nm)	
	M1	M2	M1	M2
Isopropanol	1.1×10^{-8}	7.7×10^{-9}	3.0 ± 0.1	3.0 ± 0.1
Toluene	1.7×10^{-8}	7.7×10^{-9}	3.0 ± 0.1	3.0 ± 0.1

$$P_c^* = \frac{\omega}{d_c} * \quad (1 - \frac{d_c}{d_d})^2 (1 - 2.104\left(\frac{d_c}{d_d}\right) + 2.09\left(\frac{d_c}{d_d}\right)^3 - 0.95\left(\frac{d_c}{d_d}\right)^5) \qquad (15)$$

This corrected permeability term was used in the SKK model and is plotted together with the experimental results in Fig. 5. The reflection coefficient and rejection were bounded as follows: $0 < \sigma < 1$ and $0 \leq R \leq 1$, while for the purposes of clarity and simplicity, only the Ferry pore size, as listed in Table 2, was used for d_p. This modified SKK model shows a closer fit to the experimental data, especially for M2. The better fit for M2 may be due to better approximations of the σ values, as more of the solvents of Fig. 3b reach a constant rejection value (see Fig. 3b), and, besides, the rejection of Sudan Black B in isopropanol in M1 was only tested at three pressures for membrane M1 rather than four pressures, as for membrane M2.

The modified SKK model shows that the permeability of solutes is now decreased to zero as the solute cross-sectional area nears the diffusion pore size, and that rejection is predicted past the original limit of $d_c/d_p = 1$ up to the new limit, $d_c/d_d = 1$. Fig. 5 appears to show that rejection does not approach 100% at d_d (3.0 nm), but at smaller solute sizes around $d_c = 2$ nm. This is predicted by the Renkin equation, which calculates the hindered diffusion to be 2% of its original value at $d_c/d_d = 0.66$, limiting the transport of solute across the membrane. Of course, retention experiments with molecules in the 80–100% predicted rejection range would further validate this model, though dyes molecules are generally smaller than these sizes, with Rose Bengal (M_W =973 Da) already one of the largest dyes. Additionally, grafting PDMS into the pores of ceramic membranes of various pore sizes would allow for further testing of this modified SKK model. In its present form, the modified SKK model shows that both diffusion and convection of solutes is significant and do not necessarily operate with the same (pore-size) parameters.

5. Conclusion

PDMS-grafted γ-alumina ceramic membranes showed a higher rejection of a certain solute in the presence of nonpolar solvents, such as toluene, than in more polar solvents, such as isopropanol. A relation was observed between solute rejection and the ratio of solute diameter versus membrane pore diameter, indicating that a size-exclusion mechanism is applicable to describe the membrane solute rejection when taking into account pore shrinkage due to graft swelling.

Rejection data as a function of pressure were analyzed in the frameworks applied by the Ferry, Verniory, and SHP size-exclusion models together with the Spiegler-Kedem-Katchalsky (SKK) equations to calculate pore diameters for the various solvents tested, and, subsequently, the solute permeability parameters. It was proposed that a larger pore size is experienced by the diffusion of solutes across the membranes, due to the open structure of the PDMS grafted moiety. The SKK equations were modified in response, proposing the pore size

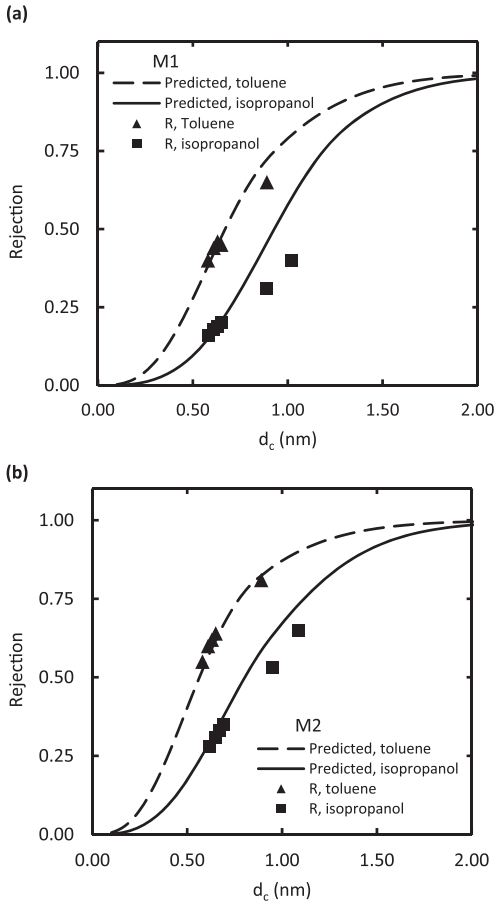

Fig. 5. Experimental and predicted dye rejection results for (a) M1 and (b) M2 in toluene and isopropanol using the modified SKK model.

available for diffusion as the pore size of γ-Al_2O_3 before PDMS grafting, as determined by permporometry measurements. This modified SKK model has a clear physical interpretation and, more importantly, offers accurate rejection predictions.

The testing of solutes of various polarities and shapes, along with solvent mixtures, would doubtless generate an additional layer of complexity when interpreting and modeling results. It remains to be seen whether the SKK model - or a derivative - could accurately predict membrane performance that involve increasingly complex solute-solvent-membrane interactions, though the insight gained from the results here certainly contributes towards understanding the fundamental mechanisms involved in solute transport across polymer-grafted ceramic membranes.

Acknowledgements

The authors acknowledge the financial support from the European Union – The Education, Audiovisual and Culture Executive Agency (EACEA) under the Program “Erasmus Mundus Doctorate in Membrane Engineering” – EUDIME (FPA 2011–2014) and an I.A.P. Grant supported by the Belgian Government under Supramolecular Analysis. This work is part of the research program titled ‘Modular Functionalized Ceramic Nanofiltration Membranes’ (BL-20-10), which is taking place within the framework of the Institute for Sustainable Process Technology (ISPT) and is jointly financed by the Netherlands Organization for Scientific Research (NWO) and ISPT.

References

[1] P. Vandezande, L.E.M. Gevers, I.F.J. Vankelecom, Solvent resistant nanofiltration: separating on a molecular level, Chem. Soc. Rev. 37 (2008) 365–405.
[2] P. Marchetti, M.F. Jimenez Solomon, G. Szekely, A.G. Livingston, Molecular separation with organic solvent nanofiltration: a critical review, Chem. Rev. 114 (2014) 10735–10806.
[3] X.Q. Cheng, Y.L. Zhang, Z.X. Wang, Z.H. Guo, Y.P. Bai, L. Shao, Recent advances in polymeric solvent-resistant Nanofiltration Membranes, Adv. Polm. Technol. 33 (2014) (n/a-n/a).
[4] K. Vanherck, G. Koeckelberghs, I.F.J. Vankelecom, Crosslinking polyimides for membrane applications: a review, Prog. Polym. Sci. 38 (2013) 874–896.
[5] P. Marchetti, M.F. Jimenez Solomon, G. Szekely, A.G. Livingston, Molecular separation with organic solvent nanofiltration: a critical review, Chem. Rev. 114 (2014) 10735–10806.
[6] S. Darvishmanesh, J. Degrève, B. Van Der Bruggen, Mechanisms of solute rejection in solvent resistant nanofiltration: the effect of solvent on solute rejection, Phys. Chem. Chem. Phys. 12 (2010) 13333–13342.
[7] X.J. Yang, A.G. Livingston, L. Freitas dos Santos, Experimental observations of nanofiltration with organic solvents, J. Membr. Sci. 190 (2001) 45–55.
[8] C. Leger, H.L. De Lira, R. Paterson, Preparation and properties of surface modified ceramic membranes. Part II. Gas and liquid permeabilities of 5 nm alumina membranes modified by a monolayer of bound polydimethylsiloxane (PDMS) silicone oil, J. Membr. Sci. 120 (1996) 135–146.
[9] R.S. Faibish, Y. Cohen, Fouling-resistant ceramic-supported polymer membranes for ultrafiltration of oil-in-water microemulsions, J. Membr. Sci. 185 (2001) 129–143.
[10] W. Yoshida, Y. Cohen, Ceramic-supported polymer membranes for pervaporation of binary organic/organic mixtures, J. Membr. Sci. 213 (2003) 145–157.
[11] W. Yoshida, Y. Cohen, Removal of methyl tert-butyl ether from water by pervaporation using ceramic-supported polymer membranes, J. Membr. Sci. 229 (2004) 27–32.
[12] K.C. Popat, G. Mor, C.A. Grimes, T.A. Desai, Surface modification of nanoporous alumina surfaces with poly(ethylene glycol), Langmuir 20 (2004) 8035–8041.
[13] L. Sang Won, S. Hao, T.H. Richard, P. Vania, U.L. Gil, Transport and functional behaviour of poly(ethylene glycol)-modified nanoporous alumina membranes, Nanotechnology 16 (2005) 1335.
[14] S. Zeidler, P. Puhlfürß, U. Kätzel, I. Voigt, Preparation and characterization of new low MWCO ceramic nanofiltration membranes for organic solvents, J. Membr. Sci. 470 (2014) 421–430.
[15] W.R. Bowen, J.S. Welfoot, Modelling the performance of membrane nanofiltration—critical assessment and model development, Chem. Eng. Sci. 57 (2002) 1121–1137.
[16] S. Blumenschein, A. Böcking, U. Kätzel, S. Postel, M. Wessling, Rejection modeling of ceramic membranes in organic solvent nanofiltration, J. Membr. Sci. 510 (2016) 191–200.
[17] S.R. Hosseinabadi, K. Wyns, A. Buekenhoudt, B. Van der Bruggen, D. Ormerod, Performance of Grignard functionalized ceramic nanofiltration membranes, Sep. Purif. Technol. 147 (2015) 320–328.
[18] S.R. Hosseinabadi, K. Wyns, V. Meynen, A. Buekenhoudt, B. Van der Bruggen, Solvent-membrane-solute interactions in organic solvent nanofiltration (OSN) for Grignard functionalised ceramic membranes: explanation via Spiegler-Kedem theory, J. Membr. Sci. 513 (2016) 177–185.
[19] E.S. Tarleton, J.P. Robinson, M. Salman, Solvent-induced swelling of membranes — measurements and influence in nanofiltration, J. Membr. Sci. 280 (2006) 442–451.
[20] C.R. Tanardi, I.F.J. Vankelecom, A.F.M. Pinheiro, K.K.R. Tetala, A. Nijmeijer, L. Winnubst, Solvent permeation behavior of PDMS grafted y-alumina membranes, J. Membr. Sci. 495 (2015) 216–225.
[21] O. Kedem, A. Katchalsky, Thermodynamic analysis of the permeability of biological membranes to non-electrolytes, Biochim. Et Biophys. Acta 27 (1958) 229–246.
[22] K. Spiegler, O. Kedem, Thermodynamics of hyperfiltration (reverse osmosis): criteria for efficient membranes, Desalination 1 (1966) 311–326.
[23] B. Van der Bruggen, Nanofiltration, in: E.M.V. Hoek, V.V. Tarabara (Eds.), Encyclopedia of Membrane Science and Technology, John Wiley & Sons, Inc, Hoboken, NJ, USA, 2013, pp. 1–22.
[24] J.D. Ferry, Ultrafilter membranes and ultrafiltration, Chem. Rev. 18 (1936) 373–455.
[25] A. Verniory, R. du Bois, P. Decoodt, J.P. Gassee, P.P. Lambert, Measurement of the permeability of biological membranes. Application to the glomerular wall, J. Gen. Physiol. 62 (1973) 489–507.
[26] S.-I. Nakao, S. Kimura, Models of membrane transport phenomena and their applications for ultrafiltration data, J. Chem. Eng. Jpn. 15 (1982) 200–205.
[27] C.R. Tanardi, A.F.M. Pinheiro, A. Nijmeijer, L. Winnubst, PDMS grafting of mesoporous γ-alumina membranes for nanofiltration of organic solvents, J. Membr. Sci. 469 (2014) 471–477.
[28] B. Van Der Bruggen, C. Vandecasteele, Modelling of the retention of uncharged molecules with nanofiltration, Water Res. 36 (2002) 1360–1368.
[29] A.F.M. Pinheiro, D. Hoogendoorn, A. Nijmeijer, L. Winnubst, Development of a PDMS-grafted alumina membrane and its evaluation as solvent resistant nanofiltration membrane, J. Membr. Sci. 463 (2014) 24–32.
[30] F.H. Allen, O. Kennard, D.G. Watson, L. Brammer, A.G. Orpen, R. Taylor, Tables of bond lengths determined by X-ray and neutron diffraction. Part 1. Bond lengths in organic compounds, J. Chem. Soc. Perkin Trans. 2 (1987) S1–S19.
[31] A. Bondi, van der Waals Volumes and Radii, J. Phys. Chem. 68 (1964) 441–451.
[32] J.L.C. Santos, P. de Beukelaar, I.F.J. Vankelecom, S. Velizarov, J.G. Crespo, Effect of solute geometry and orientation on the rejection of uncharged compounds by nanofiltration, Sep. Purif. Technol. 50 (2006) 122–131.
[33] D.R. Paul, O.M. Ebra-Lima, Pressure-induced diffusion of organic liquids through

highly swollen polymer membranes, J. Appl. Polym. Sci. 14 (1970) 2201–2224.
[34] D.R. Paul, J.D. Paciotti, O.M. Ebra-Lima, Hydraulic permeation of liquids through swollen polymeric networks. II. liquid mixtures, J. Appl. Polym. Sci. 19 (1975) 1837–1845.
[35] I.F.J. Vankelecom, K. De Smet, L.E.M. Gevers, A. Livingston, D. Nair, S. Aerts, S. Kuypers, P.A. Jacobs, Physico-chemical interpretation of the SRNF transport mechanism for solvents through dense silicone membranes, J. Membr. Sci. 231 (2004) 99–108.
[36] A.F.M. Pinheiro, A. Nijmeijer, V. Sripathi, L. Winnubst, Chemical modification/grafting of mesoporous alumina with polydimethylsiloxane (PDMS), Eur. J. Chem. 6 (2015) 287–295.
[37] A.F.M.Pinheiro, A.F.Pinheiro de Melo, Development and Characterization of Polymer-grafted Ceramic Membranes for Solvent Nanofiltration, in, GVO drukkers & vormgevers B.V. | Ponsen & Looijen, 2013.
[38] N. Petzetakis, C.M. Doherty, A.W. Thornton, X.C. Chen, P. Cotanda, A.J. Hill, N.P. Balsara, Membranes with artificial free-volume for biofuel production, Nat. Commun. 6 (2015) 7529.
[39] E.M. Renkin, Filtration, diffusion, and molecular sieving through porous cellulose membranes, J. Gen. Physiol. 38 (1954) 225–243.
[40] Z. Chen, Y. Wu, M. Zheng, J. Liu, Z. Xu, S. Zhao, C. Xu, Diffusion of sulfur-containing compounds in petroleum residue fractions I. Hindered diffusion through polycarbonate membranes at ambient conditions, Fuel 183 (2016) 99–106.
[41] R.E. Beck, J.S. Schultz, Hindered diffusion in microporous membranes with known pore geometry, Science 170 (1970) 1302–1305.
[42] A. Nacev, C. Beni, O. Bruno, B. Shapiro, The behaviors of ferro-magnetic nano-particles In and Around blood vessels under applied magnetic fields, J. Magn. Magn. Mater. 323 (2011) 651–668.